

Absolute Quantitation of Cardiac ^{99m}Tc-pyrophosphate Using Cadmium Zinc Telluride-based SPECT/CT

Sharmila Dorbala,^{abc} Mi-Ae Park,^a Sarah Cuddy,^{bc} Vasvi Singh,^b Kyle Sullivan,^a Sirwoo Kim,^a Rodney H. Falk,^c Viviany R. Taqueti,^{ab} Hicham Skali,^b Ron Blankstein,^b Camden Bay,^a Marie F. Kijewski,^a Marcelo F. Di Carli^{ab}

^a Division of Nuclear Medicine, Department of Radiology

^b CV imaging program, Cardiovascular Division

^c Cardiac Amyloidosis Program, Division of Cardiology, Department of Medicine
All at Brigham and Women's Hospital, Boston, MA 02115

Conflicts of Interest

SD: Consulting fees: Pfizer, GE Health Care; investigator-initiated grant Pfizer.

SC: Investigator-initiated research grant from Pfizer.

RHF: Consulting fees: Ionis Pharmaceuticals, Alnylam Pharmaceuticals, Caelum Biosciences
Research funding: GlaxoSmithKline, Akcea

MFD: Research grant: Spectrum Dynamics and Gilead, Consulting fees: Sanofi and GE
The other authors do not have any conflicts to declare.

Dr. Dorbala has received research support from U.S. National Institutes of Health/National Heart, Lung, and Blood Institute R01 HL130563 and HL150342 and American Heart Association grant AHA 16 CSA 28880004 for amyloidosis.

Dr. Falk has received research support from U.S. National Institutes of Health/National Heart, Lung, and Blood Institute R01 HL130563.

Address for Correspondence:

Sharmila Dorbala, MD, MPH

Division of Nuclear Medicine and Molecular Imaging, Department of Radiology
Amyloidosis Program

Brigham and Women's Hospital and Harvard Medical School

75 Francis St, Boston, MA 02115

Tel: 617-732-6290; E-mail sdorbala@bwh.harvard.edu

Twitter: @DorbalaSharmila

Word count: 5323

Abstract

Rationale: The primary aims of this study were to determine the correlation between absolute quantitative ^{99m}Tc -pyrophosphate (^{99m}Tc -PYP) metrics and traditional measures of cardiac amyloid burden and to measure intra-observer repeatability of the quantitative metrics.

Methods: We studied 72 patients who underwent ^{99m}Tc -PYP SPECT/CT using a novel general purpose CZT-based SPECT/CT system (Veriton, Spectrum Dynamics Inc). The clinical standard for these studies is visual grading (0-3: myocardial uptake none, <, =, or > rib uptake, respectively). Visual grade ≥ 2 was considered positive. For 72 patients, standardized uptake value (SUV) maximum and mean, cardiac amyloid activity (CAA; $\text{SUV}_{\text{mean}} \times \text{left ventricular (LV) volume}$), and percent injected dose (%ID) were calculated, and visual grading, was performed. Correlation of the 4 quantitative metrics and visual grades with LV mass indexed to body surface area (LVMI on echocardiography, 67 patients) was measured. For a subset of 11 patients, correlation of visual and quantitative metrics with extracellular volume (ECV on cardiac magnetic resonance imaging) was measured. Normal linear regression was used to compare the standardized association of each of the 4 quantitative metrics with LVMI, as a surrogate for amyloid burden. Receiver operating curve (ROC) analysis was used to determine the diagnostic accuracy of quantitative metrics, using visual grading as the reference standard. Intra-observer repeatability of generation of quantitative metrics was also determined.

Results: All 4 quantitative metrics were highly accurate with area under the ROC curve > 0.96 for diagnosis of ATTR cardiac amyloidosis. SUVmax, SUVmean, CAA, %ID, and visual grade were moderately positively correlated with LVMI ($r=0.485$ for ID) and strongly positively correlated, albeit in a small cohort, with ECV ($r=0.873$, SUVmax). Intraobserver repeatability was excellent with $< 2\%$ coefficient of variation for SUVmax, %ID, and CAA, and 3.8% for SUVmean. All 4 quantitative metrics had a standardized effect of > 0.324 on LVMI; the largest standardized effect was 0.485 for %ID.

Principal Conclusions: In this first study of ^{99m}Tc -PYP cardiac imaging using a novel CZT SPECT/CT scanner, SUV maximum and mean, CAA, and %ID measured by absolute quantitation of ^{99m}Tc -PYP were moderately correlated with LVMI and strongly correlated, albeit in a small

cohort, with ECV. Intra-observer repeatability of generating the quantitative metrics was excellent.

Key words (3-5): Quantitative SPECT, technetium-99m-pyrophosphate, PYP, CZT SPECT/CT

INTRODUCTION

^{99m}Tc-pyrophosphate (^{99m}Tc-PYP) has emerged as a highly specific tool to non-invasively diagnose transthyretin cardiac amyloidosis (ATTR-CA). (1) Relative ^{99m}Tc-PYP single photon emission computed tomography (SPECT) and planar imaging are the current standard for non-invasive diagnosis of ATTR-CA. ^{99m}Tc-PYP SPECT is nearly 100% specific for ATTR in patients with heart failure and typical phenotypic features of amyloidosis on echocardiography or cardiac magnetic resonance imaging (CMR) after exclusion of AL amyloidosis. (2) However, current visual grading or semi-quantitative approaches to interpretation (heart to contralateral ratio or heart to whole body ratio), while adequate for diagnosis, are inadequate for detection of early disease, identification of response to therapy, and risk assessment. Left ventricular (LV) mass by echocardiography and extracellular volume (ECV) by CMR are the current quantitative tools used to estimate cardiac amyloid burden and response to therapy. Newly developed SPECT technology with CT based attenuation correction, CZT-based detection systems with high sensitivity, as well as novel 360-degree geometry, raise the possibility of enhanced quantitative SPECT. (3)

The primary aims of this study were (1) to measure the correlation between ^{99m}Tc-PYP SPECT/CT absolute quantitative metrics, as well as visual grading, and both LV mass index (LVMI) and ECV and (2) to measure intra-observer repeatability of the quantitative metrics.

METHODS

Study Cohort and Procedures:

Consecutive patients over a six-month period with known or suspected cardiac amyloidosis referred clinically for ^{99m}Tc -PYP imaging and scanned using a general purpose CZT SPECT/CT scanner (Veriton CT, Spectrum Dynamics Inc) were included. Patients with systemic AL amyloidosis (by serum free light chain assay and serum and urine immunofixation electrophoreses) were excluded. TTR genetic testing was performed in all patients with a positive ^{99m}Tc -PYP scan. Most patients (N=67) underwent a clinical echocardiogram (median 5 days from the ^{99m}Tc -PYP scan), and a small subset of patients (N=11; 5 patients with ATTR cardiac amyloidosis and 6 patients without ATTR cardiac amyloidosis by ^{99m}Tc -PYP scan) underwent a clinical CMR study (median 61 days from the ^{99m}Tc -PYP scan). Clinical parameters, cardiac risk factors, clinical red flags for amyloidosis and risk markers of serum estimated glomerular filtration rate (eGFR) and cardiac biomarker levels (NT pro-BNP and high sensitivity troponin-T) were obtained from medical records. This study was approved by the institutional Human Research Committee.

^{99m}Tc -PYP SPECT/CT Methods:

Acquisition: A 15-min chest SPECT/CT acquisition was performed 150-180 minutes after intravenous injection of 880.6 ± 66.6 MBq (23.8 ± 1.8 mCi) of ^{99m}Tc -PYP using a Veriton-CT imaging system (Spectrum Dynamics Inc, Haifa Israel). Attenuation correction was based on a low dose non-contrast CT scan (effective mAs = 20, 120 kVP tube voltage, free tidal breathing). Radiotracer dose and patient weight were recorded to produce quantitative SPECT images. ^{99m}Tc -PYP images were reconstructed onto a 256 X 256 matrix ($2.46 \times 2.46 \times 2.46$ mm³ voxel size) by ordered subsets expectation maximization (OSEM, 4 iterations, 8 subsets), 4.48 mm full-width at half-maximum, and a proprietary filter (inter-iteration convolution filter and post median filter) with corrections for radiotracer decay, point spread function, scatter and attenuation.

Qualitative ^{99m}Tc-PYP Metrics:

^{99m}Tc-PYP SPECT images were reviewed by a single experienced physician observer, blinded to echocardiogram and CMR results, and graded using a 0-3 scale (myocardial uptake none, <, =, or > rib uptake). A visual grade ≥ 2 on CZT SPECT/CT was considered positive for a final diagnosis of ATTR.

Quantitative ^{99m}Tc-PYP Metrics:

A volume of interest (VOI) was placed on the ^{99m}Tc-PYP images using the CT scan for defining the external cardiac outline (Supplemental Figure 1). This VOI was edited on the fused ^{99m}Tc-PYP /CT images to include only LV uptake, as the right ventricular free wall activity signal was often contaminated by sternal uptake. Note that the VOI included the LV blood pool; we were not able to exclude the blood pool because CT contrast was not used, and early ^{99m}Tc-PYP blood pool data were not acquired. This approach allowed us to quantify the visually negative cases. SUV [unitless] was defined as the decay corrected activity concentration of ^{99m}Tc-PYP divided by injected activity per unit body weight. SUVmax and SUVmean were the maximum and mean activity respectively within the VOI. The product of the VOI volume and SUVmean defined integrated cardiac amyloid activity (CAA). Percent injected dose (%ID) was defined as absolute ^{99m}Tc-PYP activity concentration in the LV VOI multiplied by the VOI volume and divided by injected dose (decayed to scan start time). A single observer, blinded to other results, derived these quantitative metrics using a commercially available and validated software (MIM, Cleveland, OH) (4); measurements were repeated after 2 weeks by the same observer in a random sample of 14 studies to determine intraobserver repeatability.

CZT SPECT/CT System and Scanner Quality Control:

The 360-degree CZT SPECT/CT has 12 detector columns arranged in a circular ring with equal angular spacing. Each detector column has a 16 x 238 array of 2,048 pixelated CZT detectors for a total of 24,576 CZT detectors in the system. Each detector has a size of 2.46 x 2.46 x 6 mm³. Tungsten collimators are integrated with the CZT detectors, with square hole size of 2.46 mm, septa thickness of 0.2 mm, and hole length of 24.5 mm. To ensure full-angular sampling of

patient body, each column swivels swiveling about the its long axis and orbits counter-clockwise about the central axis of the gantry.

The SPECT/CT system was calibrated for accurate quantitation using a uniform cylindrical phantom filled with a known amount of ^{99m}Tc measured by a dose calibrator. The phantom data were reconstructed with the OSEM including attenuation and scatter correction, then the cross-calibration factor between dose calibrator and SPECT images was obtained to convert the voxel values in SPECT images into the absolute activity concentration, Bq/ml.

The stability of SPECT and CT is monitored daily using quality assurance testing prior to the first use in patient. Energy resolution, detector uniformity, count sensitivity, center of rotation, and multiple head registration of SPECT system are quantitatively measured using a Co-57 rod source. For CT, mean Hounsfield unit (HU) of water and air, standard deviation of water HU, and artifact are checked using a dedicated phantom.

Echocardiography Methods:

Clinical standard 2D echocardiography was performed as per American Society of Echocardiography recommendations. (5) Standard 2D measurements were made in triplicate; LV mass was derived using the Devereaux formula, and indexed to body surface area to derive LVMI.

Cardiac Magnetic Resonance Imaging (CMR) Methods:

Contrast enhanced CMR images were acquired on a 3.0-T system (Tim Trio, Siemens, Erlangen, Germany) as described previously. (6) Briefly, the protocol consisted of steady-state free-precession cine imaging for assessing ventricular function and morphology, and native and post-contrast T1 mapping for quantification of myocardial ECV using a modified Look-Locker technique (MOLLI 5-3-3). Segmental ECV's were calculated by the ratio of changes of relaxation rates of the myocardium to that of blood and adjusted to the fractional blood volume of distribution (1-hematocrit). Global myocardial ECV was then calculated by a single observer averaging the myocardial segmental ECV values from the short-axis slices at the base, mid, and

apical LV level. A commercial software package (MedisSuite 3.0 Medical Imaging Systems, Leiden, the Netherlands) was used to post-process and quantify ECV values. (7)

Statistics:

Data are presented as mean \pm standard deviation or medians with interquartile range as appropriate and compared using Student's t-tests and Wilcoxon rank-sum tests, respectively. Categorical variables were compared using Pearson's chi-squared tests. An ANOVA with post-hoc Bonferroni tests was used to compare quantitative ^{99m}Tc -PYP metrics by each category of visual grade. Pearson's correlation analysis was used to determine the correlation between each of the four quantitative SPECT metrics with LVMI and ECV; Spearman's correlation analysis was used for visual grading. Normal linear regression was used to determine the potential of the four quantitative metrics for prediction of LVMI. An attempt was made to utilize ridge regression to allow for the inclusion of all four highly correlated metrics in a single model. This was not successful, as one of the metrics maintained an unexpected association with LVMI unless a severe penalty was imposed. Therefore, four separate simple linear regression models were fit and the magnitude of the standardized regression coefficients, as well as R^2 , were compared among the four models. We standardized our predictors and response to allow comparison across models, as each quantitative metric is measured on a different scale. Receiver operating statistics curve (ROC) analysis was used to determine the diagnostic accuracy of SUVmax, SUVmean, CAA, and % injected dose, with visual grade-based classification as the reference standard. Unless otherwise stated, p-values less than 0.05 were considered statistically significant and all testing was two-tailed. Statistical analyses were performed using SPSS version 20.0.0 (IBM Corp., Armonk, NY).

RESULTS

The study cohort included 72 patients with known or suspected cardiac amyloidosis, 31.9% (23/72) of whom had positive ^{99m}Tc-PYP scans. The positive scans were somewhat more often grade 3 (19.4%) than grade 2 (12.5%). Patients with ATTR-CA (N=23) were older, nearly all male (22/23), experienced greater frequency of musculoskeletal symptoms (**Table 1**) and manifested a distinct cardiac phenotype on echocardiography (**Supplemental Table 1**). None of these subjects had hereditary ATTR cardiac amyloidosis.

In 6 subjects we compared planar images from NaI scanner to SPECT images on CZT SPECT/CT scanner and found perfect concordance for normal/abnormal classification. Visual grade on planar NaI was 0 (N=2), 3 (N=2), and identical on CZT SPECT/CT. In 2 participants, visual grade on planar NaI SPECT was 1 and on CZT/SPECT/CT was 0 (blood pool activity).

We evaluated the distribution of the four novel quantitative metrics of SUVmax, SUVmean, CAA, and %ID for each of the 4 visual grading categories (**Figure 1, and Supplemental Figure 2**). These metrics, in general, tracked ^{99m}Tc-PYP visual grade, and intra-observer repeatability was excellent. Area under the ROC curve was > 0.96 for each of the four quantitative metrics.

Standardized uptake value maximum (SUVmax) and SUVmean:

Figure 2 shows the distribution of SUVmax for the 4 visual grades (A), its relationships to LVMI (B) and to ECV(C), and its intraobserver repeatability (D). SUVmax was low and similar in grades 0 and 1 and high and similar in grades 2 and 3 (**Figure 2A**). SUVmax was significantly lower in patients with grades 0 and 1 combined (no ATTR cardiac amyloidosis) than in those with grade 2 and 3 combined (ATTR cardiac amyloidosis, **Table 2**). Six patients with visual grades 0 and 1 had SUVmax values suggestive of disease presence (**Figure 2A**). SUVmax was moderately positively correlated with LVMI (**Figure 2B**) and strongly positively correlated with ECV (**Figure 2C**). SUVmax was highly repeatable with a CV of 1.7%. SUVmax was strongly and positively correlated with visual grade ($r = 0.718$, $p < 0.0001$) and was highly accurate in diagnosing ATTR-CA using visual grade as reference (AUC 0.98, 95% CI 0.959-1.0).

SUVmean showed very similar findings (**Supplemental Figure 3, Table 2**). Nine patients with visual grades 0 and 1 had SUVmax values suggestive of disease presence. SUVmean was the least repeatable of the four metrics with a CV of 3.8%. SUVmean was strongly and positively correlated with visual grade ($r = 0.732$, $p < 0.0001$) and was highly accurate in diagnosing ATTR-CA using visual grade as reference (0.97, 95% CI 0.936-1.0).

Cardiac amyloid activity (CAA):

Figure 3 shows the distribution of CAA for the 4 visual grades (A), its relationships to LVMI (B) and to ECV (C), and its intraobserver repeatability (D). CAA was low and similar in patients with grades 0 and 1 and high and similar in those with grades 2 and 3 (**Table 2**). Five patients in visual grades 0 and 1 had CAA values that suggest disease presence (**Figure 3A**). CAA was moderately and positively correlated with LVMI (**Figure 3B**) and strongly and positively correlated with ECV (**Figure 3C**). CAA was highly repeatable with a CV of 2.0%. CAA was strongly and positively correlated with visual grade ($r = 0.771$, $p < 0.0001$) and was highly accurate in diagnosing ATTR-CA using visual grade as reference (0.964, 95% CI 0.927-1.0).

Percent injected dose (%ID):

Figure 4 shows the distribution of %ID for the 4 visual grades (A), its relationships to LVMI (B) and to ECV (C), and its intraobserver repeatability (D). %ID was low and similar in grades 0 and 1 and high, and similar in grades 2 and 3 (**Table 2**). Four patients in visual grade 1 had %ID values that suggest disease presence (**Figure 4A**). %ID was moderately and positively correlated with LVMI (**Figure 4B**) and strongly and positively correlated with ECV (**Figure 4C**). %ID was highly repeatable with a CV of 2.0%. %ID was strongly and positively correlated with visual grade ($r = 0.799$, $p < 0.0001$), and was highly accurate in diagnosing ATTR-CA using visual grade as reference (AUC 0.97, 95% CI 0.946-1.0).

Visual grade:

Visual grade was moderately and positively correlated with LVMI ($r = 0.394$, $p = 0.001$) and strongly and positively correlated with ECV (0.787 , $p = 0.004$).

Predictors of LVMI:

We performed normal linear regression analyses of each of the four quantitative metrics against LVMI (**Table 3**); ECV was not included due to the small sample size. We standardized our predictor and response to allow for comparison among metrics. Regression coefficients for all metrics were statistically significantly different than 0 with $p < 0.001$ for SUVmax, CAA, and %ID, and $p = 0.007$ for SUVmean. All R^2 values were greater than 0.104, with %ID having the highest at 0.235. %ID had the highest standardized coefficient (0.485 with 95% CI 0.269-0.701).

DISCUSSION

We report several notable findings in this pilot study of quantitative ^{99m}Tc -PYP imaging using a novel general purpose CZT scanner with 360-degree detector geometry. First, continuous quantitative measures of SUVmax, SUVmean, CAA, and %ID were similarly low in patients with visual grades 0/1 and similarly high in those with grades 2/3. SUVmax, SUVmean, %ID, and CAA, as well as visual grade, were moderately positively correlated with LVMI and strongly positively correlated, albeit in a small sample, with ECV. ^{99m}Tc -PYP visual grade correlates moderately with LVMI and strongly with ECV. Our sample size was not large enough to allow comparison of correlation coefficients among metrics, but the results suggest that SUVmean was inferior to other quantitative metrics in terms of correlation with LVMI and intraobserver repeatability. This is not surprising, as SUVmean is the metric that is most sensitive to VOI definition. Our results also suggest that %ID was stronger than the other three metrics in predicting amyloid burden by LVMI.

In this study, quantitative ^{99m}Tc -PYP measures were consistent with visual grade. Some patients in grades 0 and 1 had quantitative values similar to that of the patients diagnosed with ATTR-CA, suggesting that quantitative SPECT has the potential to provide more granular information to diagnose amyloidosis compared to visual grade. Our results align with, and add to, prior reports on ^{99m}Tc -DPD (^{99m}Tc -labelled 3,3-diphosphono-1,2-propanodicarboxylic acid) with latest scanners in small cohorts, (8) and using % injected dose and older generation SPECT/CT scanners with ECV correlation in larger cohort, (9) showing similar quantitative measures in visual grade 0/1 and visual grade 2/3. Advances in SPECT instrumentation and software, notably CT-based attenuation correction, high-sensitivity 360-degree CZT-based scanners, and improved reconstruction algorithms, may further improve accuracy of SPECT with absolute quantitation. (10)

Sensitivity of the CZT SPECT system in a standard size patient is about 10% higher than that of NaI(Tl)-based gamma camera. (11) CZT camera also offers slightly improved resolution compared to NaI(Tl) camera. It has been shown that dead-time losses at high count rate are negligible for CZT camera for the activity range in clinical exams. (12) In principle these results can be extrapolated to other CZT SPECT/CT systems but that remains to be studied further.

The results of the ROC analysis indicate that all 4 quantitative metrics were highly accurate for diagnosis of ATTR amyloidosis using visual grade as reference standard; however, there are limitations to this analysis. Visual grading is based on the same images used to derive quantitative metrics; this lack of independence ensures high performance. Furthermore, our data suggest that the quantitative metrics may be superior to the reference standard, visual grading, in diagnostic performance.

In a large multicenter study, Gillmore et al. (2) evaluated the diagnostic accuracy of ^{99m}Tc -PYP/DPD /HMDP(hydroxy-methane-diphosphonate) in relation to endomyocardial biopsy and reported that a visual grade of 2/3 was highly specific (nearly 100% specific) for diagnosing ATTR-CA in patients with heart failure and typical echocardiographic or CMR features of amyloidosis if a monoclonal process is excluded. However, in other studies, the visual grade was not an independent predictor of prognosis; (13,14) semi-quantitative measures of ^{99m}Tc -PYP or DPD,

including high heart to contralateral ratio (13) and high heart to whole body ratio, (15) showed independent value to predict worse survival. Similarly, we expect ^{99m}Tc -PYP absolute quantitative metrics, including SUVmax, SUVmean, cardiac amyloid activity, and %ID, to play an important role in risk assessment.

Quantitative ^{99m}Tc -PYP imaging offers a specific molecular signal of amyloidosis that is likely to play an important role in the detection of early disease and in the assessment of response to novel TTR stabilizing (16) or novel TTR silencing therapies. Whether the grade 0 and 1 patients with higher quantitative metrics, in this cohort, represent early ATTR-CA is difficult to ascertain, as this study was based on a referral cohort of patients with heart failure. Screening of a community-based cohort of older individuals for age-related wild type ATTR-CA using ^{99m}Tc -PYP imaging with longitudinal follow-up, or hereditary ATTR patients for development of hereditary ATTR-CA, or correlative studies with ECV, would be a better study design to evaluate the value of quantitative metrics in early disease detection.

Our results demonstrate, in a small cohort, a strong correlation of quantitative ^{99m}Tc -PYP metrics with ECV, a sensitive and quantitative measure of cardiac amyloid burden that has served as a marker of prognosis in AL (17) and ATTR (18) cardiac amyloidosis. As in our study, Ross et al.(9) demonstrated similarly high correlations of ^{99m}Tc -DPD %ID and ECV in 44 patients. Together these two studies support the value of %ID of ^{99m}Tc -PYP and DPD in estimating cardiac amyloid burden; larger studies are warranted.

In this study we evaluated four quantitative metrics: SUVmax —representing a single voxel value; SUVmean—mean of all voxels in the LV VOI; CAA—the product of SUVmean and LV volume; and %ID— the product of mean activity concentration within the LV VOI and its volume, normalized to injected dose. Three of the four quantitative metrics showed high repeatability, suggesting their utility to evaluate response to therapy. Of the quantitative metrics studied, SUVmax is of limited value, as it is determined by a single voxel value in the entire VOI and can be contaminated by spillover from overlapping bone activity. SUVmean is an average over the entire LV (and blood pool) and may better represent burden of ATTR-CA, but this metric may be insensitive to early disease which may start focally; furthermore, it is very sensitive to VOI definition and, therefore,

less repeatable than the other metrics. CAA and %ID metrics are volumetric metrics that take into account myocardial volume. Although SUVmax and SUVmean performed as well as CAA and %ID in terms of correlation to standard metrics of amyloid burden, the latter metrics may prove superior for risk stratification and assessment of response to therapy. Finally, SUVmax, SUVmean, and CAA incorporate normalization to body weight, which is not optimal for highly specific tracers. This may be a factor in the apparent superiority of %ID.

This observational study included a small number of patients with ECV, the current reference standard for amyloid burden. Previously studied ^{99m}Tc -PYP metrics, i.e., heart to whole body retention index and heart to contralateral ratio, were not evaluated in this study, as early imaging and planar imaging data, respectively, were not available. High SUVmax in patients with visual grades 0, and 1 could represent excess blood pool activity, but that is less likely as the duration between injection and scan was 150-180 minutes. Despite these limitations, this study of 72 patients is the largest report to date on quantitative ^{99m}Tc -PYP SPECT/CT (8) and, to the best of our knowledge, the first report on quantitative ^{99m}Tc -PYP imaging using a 360-degree CZT SPECT/CT with advanced reconstruction algorithms.

In conclusion, absolute quantitative metrics derived from ^{99m}Tc -PYP SPECT/CT images are moderately to strongly correlated with traditional structural markers of cardiac amyloid burden and, furthermore, SUVmax, CAA, and %ID are highly repeatable. Cardiac amyloid activity and percent injected dose are promising tomographic quantitative metrics of cardiac amyloid burden; future studies validating their role for detection of early disease, assessment of response to therapy, and risk stratification are warranted.

Acknowledgements: We are grateful to Christopher Breault for his help with image export and image analysis training.

KEY POINTS:

QUESTION: Can myocardial amyloid burden be quantified using ^{99m}Tc -pyrophosphate imaging using advanced CZT SPECT/CT scanner technology with a 360-degree detector configuration?

PERTINENT FINDINGS: In a cohort study of 72 persons with known or suspected cardiac amyloidosis undergoing quantitative ^{99m}Tc -PYP CZT-SPECT/CT imaging, we found that absolute quantitative metrics derived from ^{99m}Tc -PYP images are moderately to strongly correlated with traditional structural markers of cardiac amyloid burden on echocardiography (N=67) or cardiac magnetic resonance imaging (N=11) and highly repeatable.

IMPLICATIONS FOR PATIENT CARE: Quantitative ^{99m}Tc -PYP SPECT/CT offers the potential for early detection, risk stratification, and monitoring of response to therapy in patients with cardiac amyloidosis.

References:

1. Dorbala S, Ando Y, Bokhari S, et al. ASNC/AHA/ASE/EANM/HFSA/ISA/SCMR/SNMMI expert consensus recommendations for multimodality imaging in cardiac amyloidosis: Part 1 of 2-evidence base and standardized methods of imaging. *J Nucl Cardiol*. 2019.
2. Gillmore JD, Maurer MS, Falk RH, et al. Nonbiopsy Diagnosis of Cardiac Transthyretin Amyloidosis. *Circulation*. 2016;133:2404-2412.
3. Hutton BF, Erlandsson K, Thielemans K. Advances in clinical molecular imaging instrumentation. *Clinical and Translational Imaging*. 2018;6:31-45.
4. Dibble EH, Alvarez AC, Truong MT, Mercier G, Cook EF, Subramaniam RM. 18F-FDG metabolic tumor volume and total glycolytic activity of oral cavity and oropharyngeal squamous cell cancer: adding value to clinical staging. *J Nucl Med*. 2012;53:709-715.
5. Mitchell C, Rahko PS, Blauwet LA, et al. Guidelines for Performing a Comprehensive Transthoracic Echocardiographic Examination in Adults: Recommendations from the American Society of Echocardiography. *J Am Soc Echocardiogr*. 2019;32:1-64.
6. Cuddy SAM, Bravo PE, Falk RH, et al. Improved Quantification of Cardiac Amyloid Burden in Systemic Light Chain Amyloidosis: Redefining Early Disease? *JACC Cardiovasc Imaging*. 2020;13:1325-1336.
7. Fujita N, Duerinckx AJ, Higgins CB. Variation in left ventricular regional wall stress with cine magnetic resonance imaging: normal subjects versus dilated cardiomyopathy. *Am Heart J*. 1993;125:1337-1345.
8. Caobelli F, Braun M, Haaf P, Wild D, Zellweger MJ. Quantitative (99m)Tc-DPD SPECT/CT in patients with suspected ATTR cardiac amyloidosis: Feasibility and correlation with visual scores. *J Nucl Cardiol*. 2019.
9. Ross JC, Hutt DF, Burniston M, et al. Quantitation of 99mTc-DPD uptake in patients with transthyretin-related cardiac amyloidosis. *Amyloid*. 2018;25:203-210.
10. Bailey DL, Willowson KP. An evidence-based review of quantitative SPECT imaging and potential clinical applications. *J Nucl Med*. 2013;54:83-89.

- 11.** Desmots C, Bouthiba MA, Enilorac B, Nganoa C, Agostini D, Aide N. Evaluation of a new multipurpose whole-body CzT-based camera: comparison with a dual-head Anger camera and first clinical images. *EJNMMI Phys.* 2020;7:18.
- 12.** Erlandsson K, Kacperski K, van Gramberg D, Hutton BF. Performance evaluation of D-SPECT: a novel SPECT system for nuclear cardiology. *Phys Med Biol.* 2009;54:2635-2649.
- 13.** Castano A, Haq M, Narotsky DL, et al. Multicenter Study of Planar Technetium 99m Pyrophosphate Cardiac Imaging: Predicting Survival for Patients With ATTR Cardiac Amyloidosis. *JAMA Cardiol.* 2016.
- 14.** Hutt DF, Fontana M, Burniston M, et al. Prognostic utility of the Perugini grading of 99mTc-DPD scintigraphy in transthyretin (ATTR) amyloidosis and its relationship with skeletal muscle and soft tissue amyloid. *Eur Heart J Cardiovasc Imaging.* 2017;18:1344-1350.
- 15.** Rapezzi C, Quarta CC, Guidalotti PL, et al. Role of (99m)Tc-DPD scintigraphy in diagnosis and prognosis of hereditary transthyretin-related cardiac amyloidosis. *JACC Cardiovasc Imaging.* 2011;4:659-670.
- 16.** Maurer MS, Schwartz JH, Gundapaneni B, et al. Tafamidis Treatment for Patients with Transthyretin Amyloid Cardiomyopathy. *N Engl J Med.* 2018;379:1007-1016.
- 17.** Banyersad SM, Fontana M, Maestrini V, et al. T1 mapping and survival in systemic light-chain amyloidosis. *Eur Heart J.* 2015;36:244-251.
- 18.** Martinez-Naharro A, Kotecha T, Norrington K, et al. Native T1 and Extracellular Volume in Transthyretin Amyloidosis. *JACC Cardiovasc Imaging.* 2019;12:810-819.

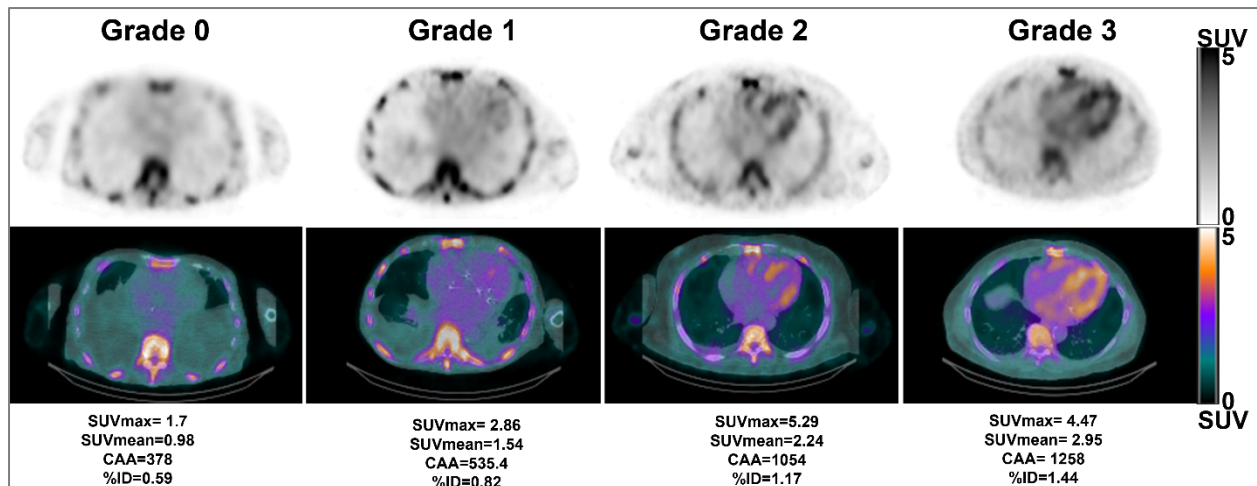


Figure 1: Representative ^{99m}Tc -PYP SPECT/CT images on an SUV scale showing grade 0, grade 1, grade 2 to grade 3 uptake (from left to right columns). The top row shows attenuation corrected SPECT images; the middle row shows SPECT/CT fusion images; and the bottom row shows the corresponding SUVmax, SUVmean, CAA, and %ID values for each image. Abbreviations for this and the other figures: SUV = standardized uptake value; max = maximum; CAA = cardiac amyloid activity; ID = injected dose.

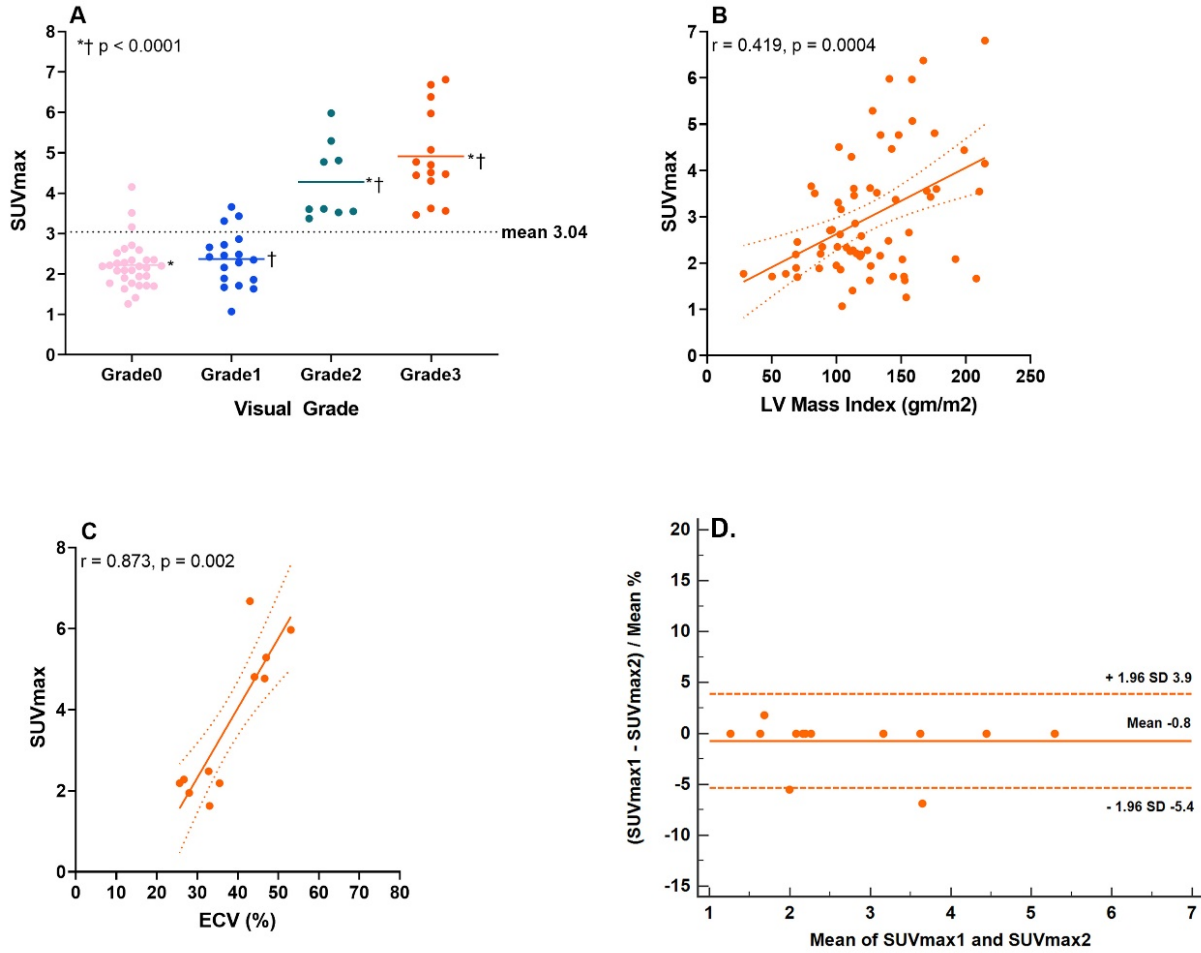


Figure 2: ^{99m}Tc -PYP SUVmax distribution by visual grade (A), its correlation to LVMI (B), its correlation to ECV (C), and its repeatability using Bland Altman plots (D). SUVmax was similar in grade 0 and grade 1, and similar but higher in grade 2 and grade 3. Correlation to LVMI (N=67) was moderate, and correlation to ECV (N=11) was strong. Bland Altman plots show excellent repeatability with a CV of 1.7%. For this and for figures 3-4: CV = coefficient of variation; LVMI = left ventricular mass index; ECV = extracellular volume. The dotted line in (A) represents mean values for the entire study cohort, in B and C indicate standard error and in C indicates standard deviation.

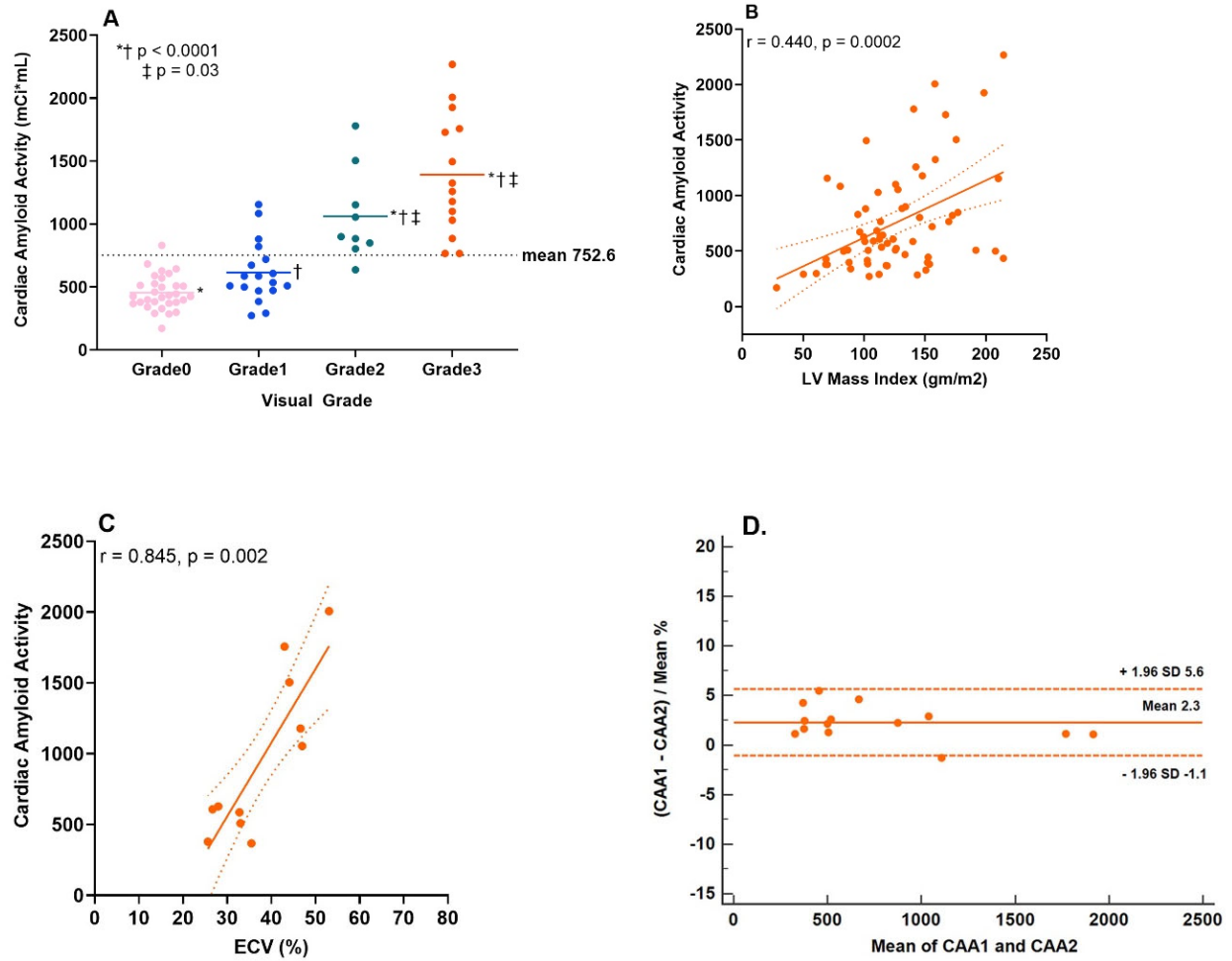


Figure 3: ^{99m}Tc-PYP cardiac amyloid activity (CAA) distribution by visual grade (A), its correlation to LVMI (B), its correlation to ECV (C), and its repeatability using Bland Altman plots (D). CAA was similar in grade 0 and grade 1, and similar but higher in grade 2 and grade 3) Correlation to LVMI (N=67) was moderate, and correlation to ECV (N=11) was strong. Bland Altman plots show excellent repeatability with a CV of 2.0%.

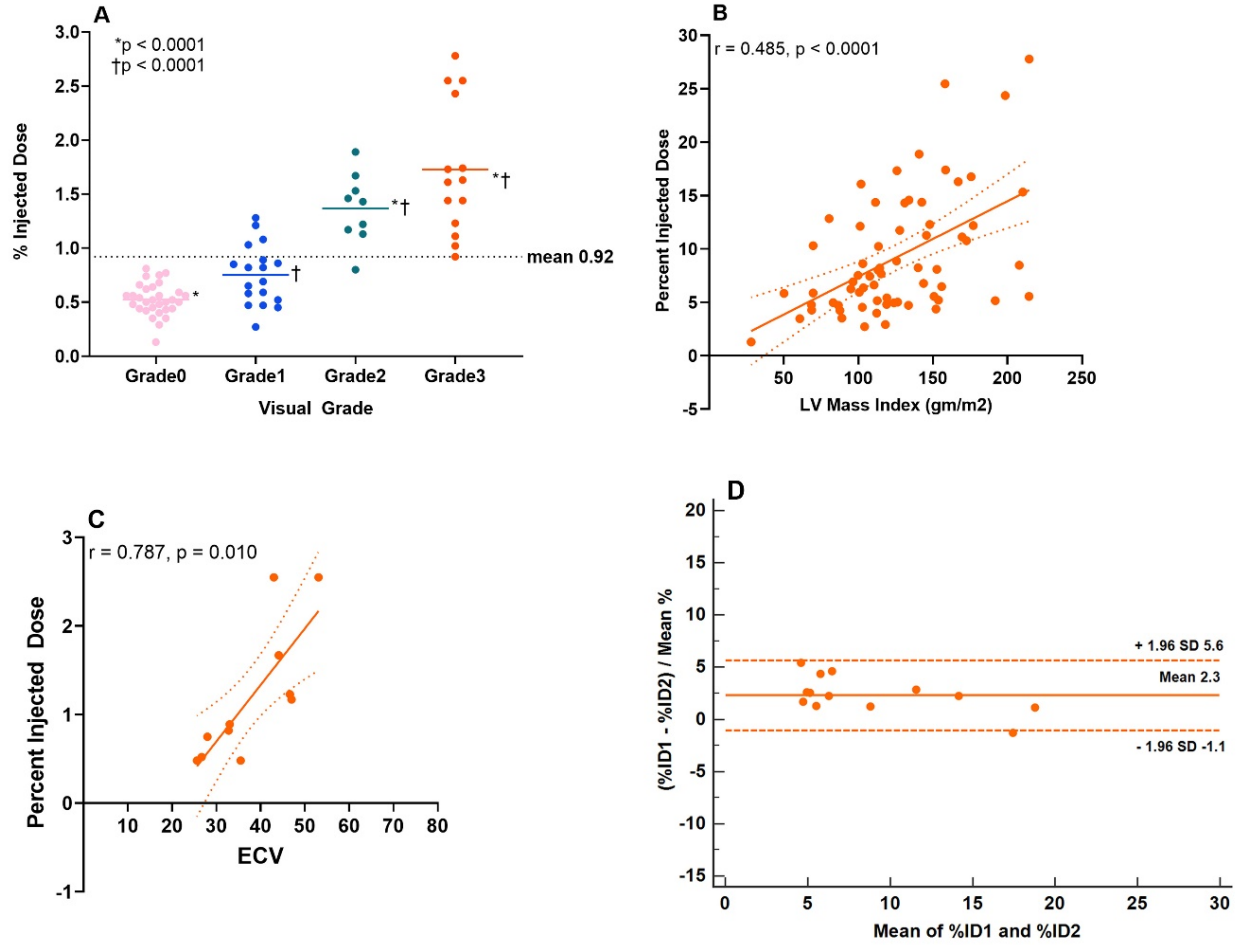


Figure 4: ^{99m}Tc -PYP percent injected dose (%ID) distribution by visual grade (A), its correlation to LVMI (B), its correlation to ECV (C), and its repeatability using Bland Altman plots (D). %ID was similar in grade 0 and grade 1, and similar but higher in grade 2 and grade 3. Correlation to LVMI (N=67) was moderate, and correlation to ECV (N=11) was strong. Bland Altman plots show excellent repeatability with a CV of 2.0%.

Table 1. Baseline Characteristics

	No-ATTR-CA (N = 49)	ATTR-CA (N = 23)	p-value
Demographics			
Age, mean \pm SD, years	73.7 \pm 11.0	81.3 \pm 8.1	0.004
Male, N (%)	32 (65.3)	22 (95.7)	0.006
Body surface area, mean \pm SD, kg/m ²	2.04 \pm 0.29	1.95 \pm 0.18	0.06
White, N (%)	37 (82.2)	21 (95.5)	0.136
Black, N (%)	8 (17.8)	1 (4.5)	0.136
Risk Factor History			
Hypertension, N (%)	43 (89.6)	21 (91.3)	0.820
Hyperlipidemia, N (%)	33 (70.2)	19 (82.6)	0.265
Heart failure, N (%)	41 (83.7)	20 (87)	0.718
Coronary artery disease, N (%)	18 (34.6)	11 (50)	0.324
Diabetes, N (%)	20 (41.7)	10 (43.5)	0.885
Smoking, N (%)	22 (45.8)	13 (56.5)	0.399
Pedal edema, N (%)	26 (54.2)	10 (45.5)	0.498
Stroke, N (%)	7 (14.6)	7 (30.4)	0.116
Musculoskeletal, † N (%)	14 (30.4)	19 (82.6)	<0.0001
New York Heart Association Class \geq II, N (%)	31 (64.5)	18 (78.3)	0.623

LV=left ventricular; IQR = interquartile range; *not reported in patients with atrial fibrillation.

SUV = standardized uptake value; ID = injected dose; CAA = cardiac amyloid activity.

†Musculoskeletal includes carpal tunnel syndrome, biceps tendon rupture, lumbar spinal stenosis.

Table 2. Quantitative ^{99m}Tc-PYP Imaging Metrics

Imaging Metric	No-ATTR-CA (N = 49)	ATTR-CA (N = 23)	p-value
SUVmean, mean ± SD, %	1.3 ± 0.3	2.4 ± 0.6	<0.0001
SUVmax, mean ± SD, %	2.3 ± 0.6	4.7 ± 1.1	<0.0001
CAA, mean ± SD, %	513 ± 196	1263 ± 461	<0.0001
%ID, mean ± SD, %	0.61 ± 0.23	1.59 ± 0.54	<0.0001

SUV = standardized uptake value; ID = injected dose; CAA = cardiac amyloid activity.

Table 3. Linear regression analyses

Models	Dependent Variable	Independent variables	R²	Standardized coefficient (95% CI)	t	p
1	LVMI	SUVmax	0.175	0.419 (0.193-0.645)	3.716	< 0.001
2	LVMI	SUVmean	0.105	0.324 (0.090-0.558)	2.761	0.007
3	LVMI	CAA	0.194	0.440 (0.218-0.662)	3.953	< 0.001
4	LVMI	%ID	0.235	0.485 (0.269-0.701)	4.474	< 0.001

SUV = standardized uptake value; CAA = cardiac amyloid activity; ID = injected dose; LVMI = left ventricular mass index.

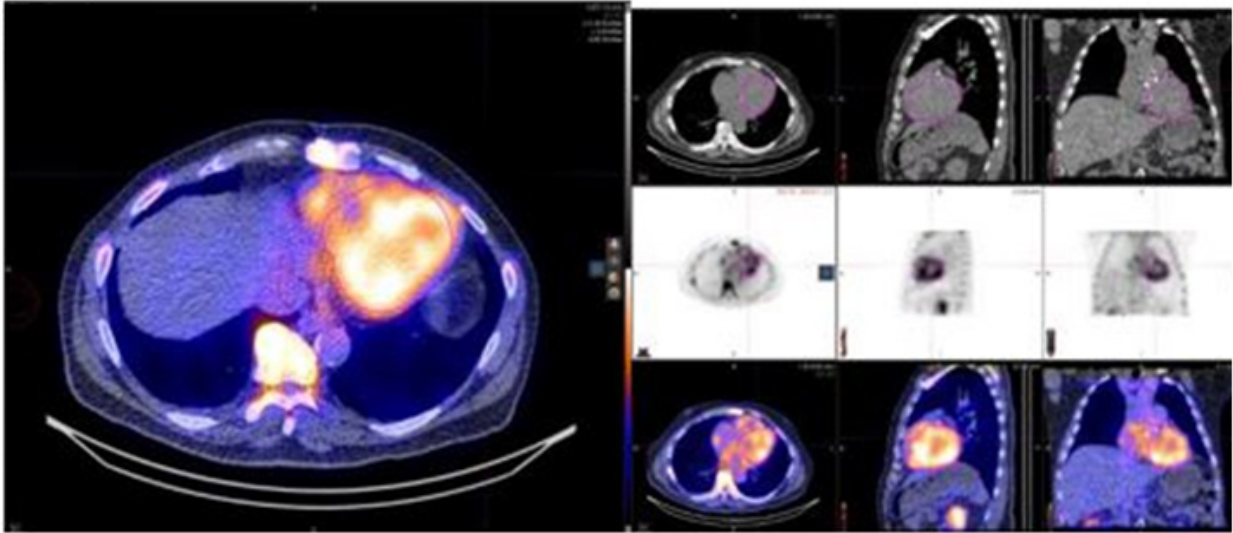
SUPPLEMENTAL MATERIAL

Results:

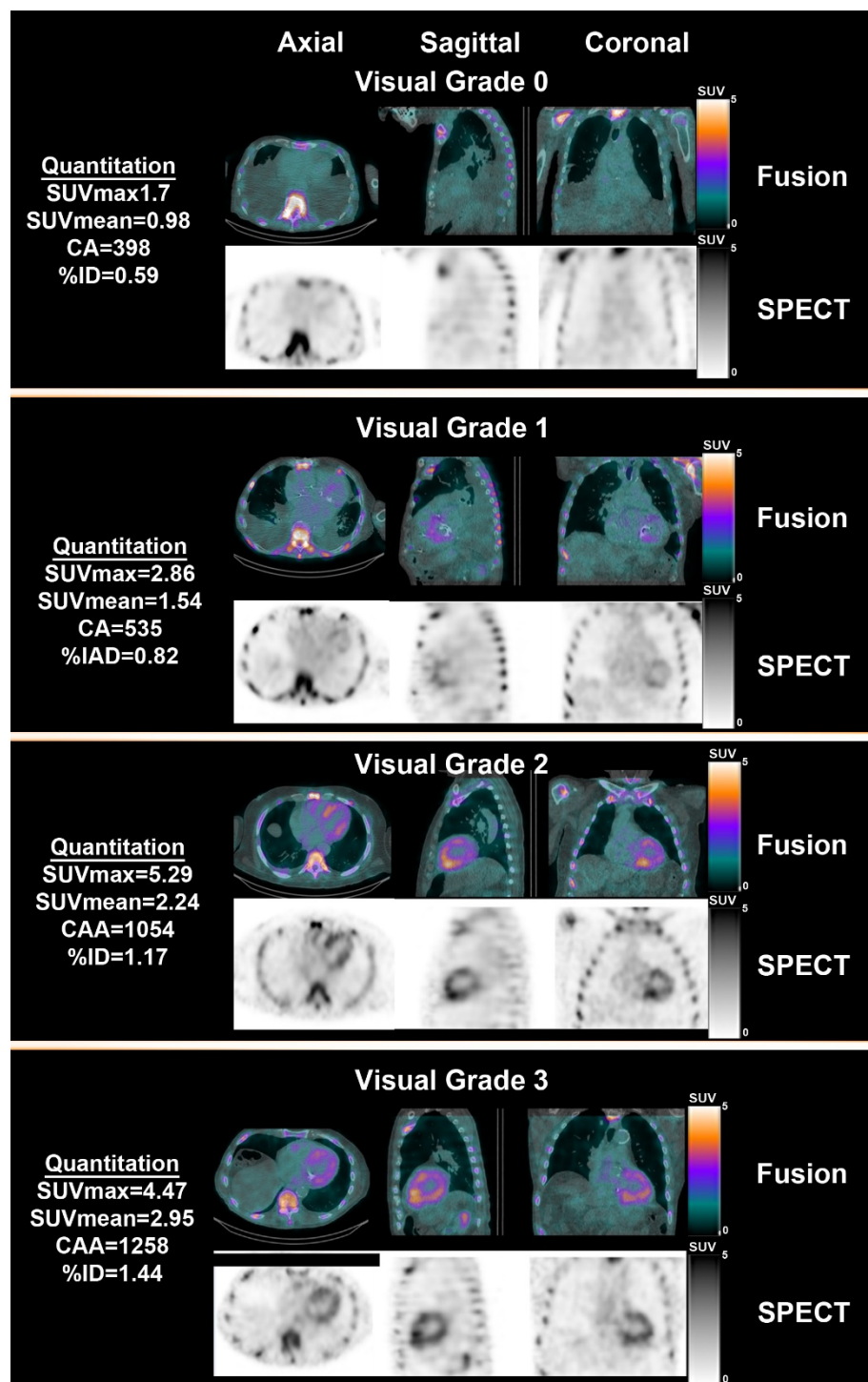
Supplemental Table 1. Laboratory and echocardiographic features

	No-ATTR-CA (N = 49)	ATTR-CA (N = 23)	p-value
Laboratory			
Estimated glomerular filtration rate, mL/gm/min, mean ± SD,	50.7 ± 21.0	55.8 ± 19.9	0.351
Troponin T, median (IQR), ng/mL,	36.5 (15.5-73.8)	57.0 (33-70)	0.051
NT-proBNP, median (IQR), pg/mL	1395 (291-3569)	3753 (2142-5682)	0.001
Echocardiography			
LV ejection fraction, mean ± SD, %	58.0 ± 10.2	51.6 ± 12.1	0.07
LV end diastolic diameter, mean ± SD, cm	4.2 ± 1.3	4.0 ± 1.0	0.351
LV end systolic diameter, mean ± SD, cm	2.9 ± 1.1	3.0 ± 1.0	0.841
Interventricular septal thickness, mean ± SD, cm	1.2 ± 0.4	1.7 ± 0.5	<0.0001
Posterior wall thickness, mean ± SD, cm	1.2 ± 0.4	1.5 ± 0.5	0.008
E, mean ± SD, m	0.9 ± 0.4	1.0 ± 0.3	0.423
A, mean ± SD, m*	0.7 ± 0.4	0.4 ± 0.3	0.01
e' lateral, mean ± SD, m	0.07 ± 0.03	0.05 ± 0.02	0.03
Tricuspid Annular Plane Systolic Excursion, mean ± SD, mm	17.0 ± 6.3	14.1 ± 4.8	0.068

NT-proBNP=N-terminal pro-brain natriuretic peptide.



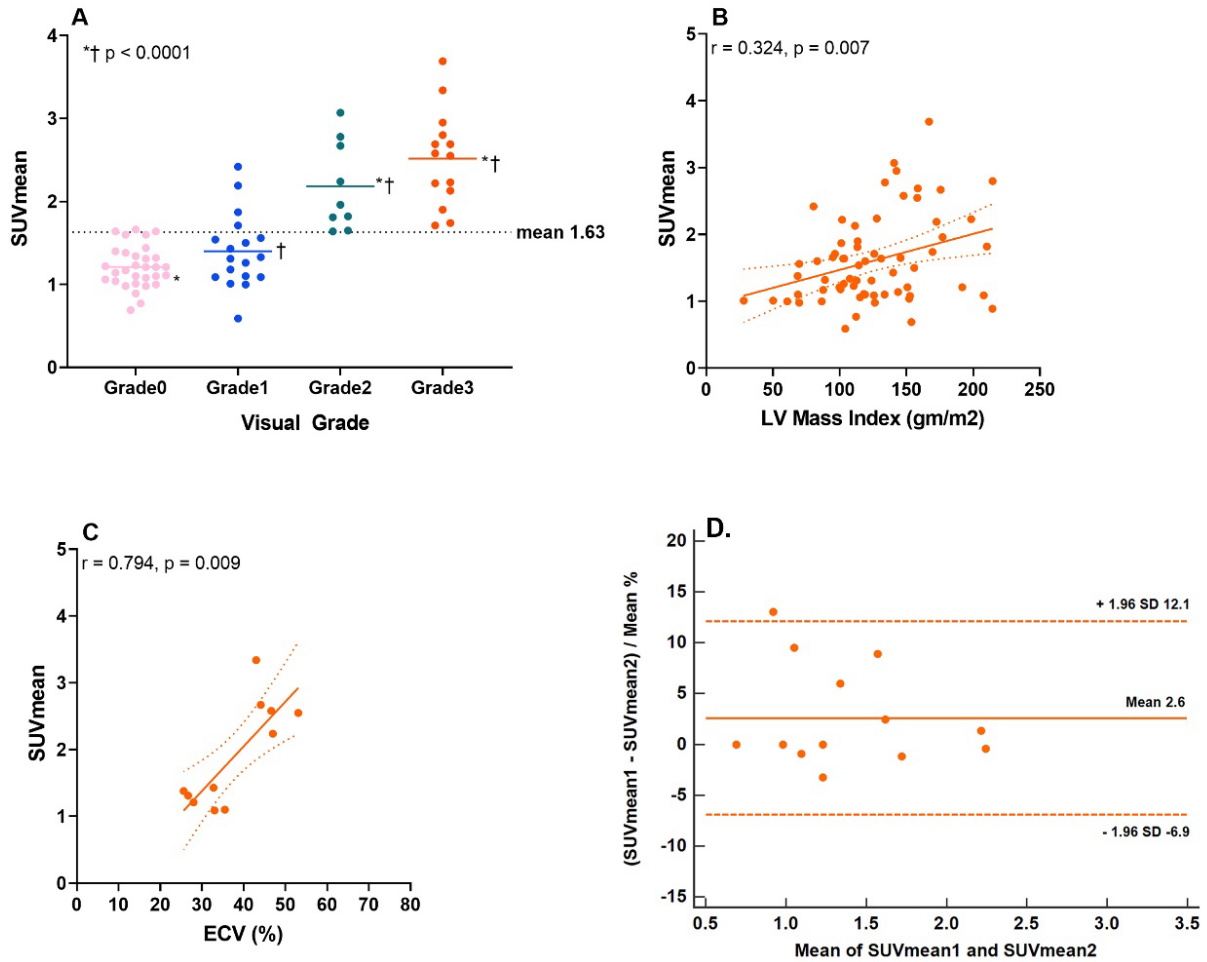
Supplemental Figure 1: An image illustrating the use of MIM software to define myocardial definition for SUV calculations using the cardiac borders on the CT scan to define the region of interest.



Supplemental Figure 2: Representative ^{99m}Tc -PYP SPECT/CT image panels showing grade 0, grade 1, grade 2 to grade 3 uptake (top to bottom panels) and coronal, axial and sagittal images (from left to right). In each panel, the top row shows attenuation corrected SPECT images and the bottom row shows SPECT/CT fusion images. On the left are listed the corresponding

SUVmax, SUVmean, CAA, and %ID values for each image. Abbreviations for this and the other figures: SUV = standardized uptake value; max = maximum; CAA = cardiac amyloid activity; ID = injected dose.

Figure 3. Performance characteristics of SUVmean



Supplemental Figure 3: ^{99m}Tc-PYP SUVmean distribution by visual grade (A), its correlation to LVMI (B), its correlation to ECV (C), and its repeatability using Bland Altman plots (D). SUVmean was similar in grade 0 and grade 1, and similar but higher in grade 2 and grade 3. Correlation to LVMI (N=67) was moderate, and correlation to ECV (N=11) was strong. Bland Altman plots show good repeatability with a CV of 3.8 %. CV = coefficient of variation; LVMI = left ventricular mass index; ECV = extracellular volume. The dotted line in (A) represents mean values for the entire study cohort, in B and C indicate standard error and in C indicates standard deviation.